J. Fluid Mech. (1970), *vol.* 42, *part* 1, *pp.* 161–175
Printed in Great Britain

Non-linear effects in a Rayleigh–Bénard experiment

By D. R. CALDWELL

Institute of Geophysics and Planetary Physics
University of California, San Diego†

(Received 22 October 1969)

Observations of temperature drop as a function of heat flow in Rayleigh–Bénard convection with curved density profiles show: (1) reversal of slope in the heating curve, (2) oscillations with time, (3) history dependence, and (4) an increase in critical Rayleigh number as the curvature of the density profile is increased. Some of the results are quite similar to the predictions of Busse.

Introduction

Some recent theoretical studies of Rayleigh–Bénard convection have shown that the temperature difference across the fluid layer is not always an increasing function of the heat flux. Certain circumstances, such as boundary conditions, variations of fluid properties with temperature, concentration gradients, or time variation of the heat flux, can allow the temperature difference, ΔT, to decrease as the heat flux is increased within a limited range in heat flux. ΔT may be multiple-valued and the state of the system may depend on its history. In these cases the convective motion is initiated by finite amplitude disturbances which cannot be described by the linearized perturbation theory used to calculate the growth of infinitesimal perturbations, or by 'overstable' (oscillatory) modes.

Veronis (1965) showed that in the presence of a stabilizing solute concentration gradient, finite amplitude disturbances can initiate convective flow at Rayleigh numbers far smaller than those necessary for transition due to infinitesimal disturbances. Figure 4 of his paper shows the multiple-valued heating curve resulting.

Busse (1967) considered a situation where the heat flux is the given parameter (rather than ΔT), and where the fluid properties vary appreciably with temperature (but no solute is present) and showed that finite amplitude disturbances can induce convection at Rayleigh numbers smaller than required for infinitesimal perturbations. He found that oscillatory states are possible, and his predicted heating curves, shown schematically in his figure 1, are multiple-valued when the Rayleigh number is near 'critical'.

Veronis (1963) also considered the case of fresh water near the maximum density point and found a similar heating curve and the possibility of finite amplitude instability at Rayleigh numbers subcritical according to the linearized theory.

† Present address: Department of Oceanography, Oregon State University, Corvallis Oregon.

Krishnamurti (1968*a*) found that changing the heat flux with time can make a multiple-valued heating curve possible. Her calculated curve (figure 2 of her paper) is quite similar to that of Busse. Oscillations are also expected in this case.

All of these studies show certain common features; a dip in the heat transfer curve just above the onset of convection and non-steady motion at this point. The only experimental observation of these effects is Krishnamurti's (1968*b*) for time-dependent heat flux. Both hysteresis and oscillation were seen in the heating curves, but the experiment was not intended to be quantitatively accurate.

In this paper an experiment is described which resembles most closely the situation described by Busse. All measurements were made with the system in a steady state, except for self-induced oscillations. No concentration gradients were present initially, although it is possible that the heat flux might induce a solute concentration gradient by means of the Soret effect, which might be either stabilizing or destablizing, as discussed below. The given parameter was the heat production in a layer below the fluid, not ΔT. At times the coefficient of thermal expansion varied by more than 20 % across the fluid layer, so the variation of fluid properties was significant.

The effects described here were discovered during the course of an experiment designed to use observations of the critical Rayleigh number in sea water to measure its coefficient of thermal expansion β. According to the linearized perturbation theory (as described in Chandrasekhar (1961)), convection begins when the Rayleigh number, R, reaches its critical value: i.e. when

$$R = \frac{\rho^2 c_p g \beta \Delta T d^3}{\mu k} \equiv R_c$$

(the symbols are defined in table 1).

For a fluid of constant properties confined between rigid horizontal boundaries maintained at constant temperatures, $R_c = 1708$. The apparatus was designed to measure the ΔT corresponding to R_c so that β could be calculated, using better known properties of the fluid. ΔT_c is defined as the value of ΔT when the ΔT *vs.* heat flow (Q) (which will be called the heating curve) changes slope, and β is then calculated as

$$\beta = \frac{\mu k R_c}{\rho^2 c_p g d^3 \Delta T_c},$$

where R_c is assumed to be 1708. The experiment was run twenty-seven times at twenty-three different pressure-temperature points. In runs where the pressure was over 300 bars, and in the higher temperature runs, the heating curves closely resembled those obtained by others (such as Schmidt & Milverton 1935; Malkus 1954; Silverston 1958). One example is shown as figure 1. The data points lie on two straight lines. For small Q, ΔT is just proportional to Q since the heat is carried by conduction alone. (This section of the plot will be called the conduction line.) At larger Q the points lie on another straight line, which has a smaller slope because some heat is now carried by convection. The value of ΔT at which the two lines meet is taken as ΔT_c. The results of these measurements agree quite closely with values of β calculated from the formulate for specific volume given by Lafond (1951).

Symbol	Quantity	Units	Value			
			0 °C		20 °C	
			1 bar	1000 bars	1 bar	1000 bars
β	Coefficient of thermal expansion	$(°C)^{-1}$	5×10^{-5}	26×10^{-5}	26×10^{-5}	36×10^{-5}
μ	Viscosity	Poise	0·0188	0·0186	0·0108	0·0103
k	Thermal conductivity	cal/sec cm °C	$1{\cdot}34 \times 10^{-3}$	$1{\cdot}41 \times 10^{-3}$	$1{\cdot}42 \times 10^{-3}$	$1{\cdot}49 \times 10^{-3}$
ρ	Density	cm^3/g	0·9726	0·9337	0·9757	0·9396
c_p	Specific heat at constant pressure	cal/g °C	1·19	1·15	1·19	1·15
x	Thermal diffusivity	cm^2/sec	$1{\cdot}39 \times 10^{-3}$	$1{\cdot}46 \times 10^{-3}$	$1{\cdot}49 \times 10^{-3}$	$1{\cdot}57 \times 10^{-3}$
ν	Kinematic viscosity	cm^2/sec	0·0183	0·0166	0·0105	0·0102
σ_T	Soret coefficient	$(°C)^{-1}$	?	?	?	?
d	Thickness of fluid layer	cm	—	—	0·635	—

TABLE 1

When the pressure and temperature both were low, however, the heating curve had quite a different appearance, and the observed values of R_c changed. Under these conditions ΔT actually decreased as Q was increased at the transition point. In one case an *increase* of 0·27 % in Q produced a *decrease* of 1·98 % in ΔT.

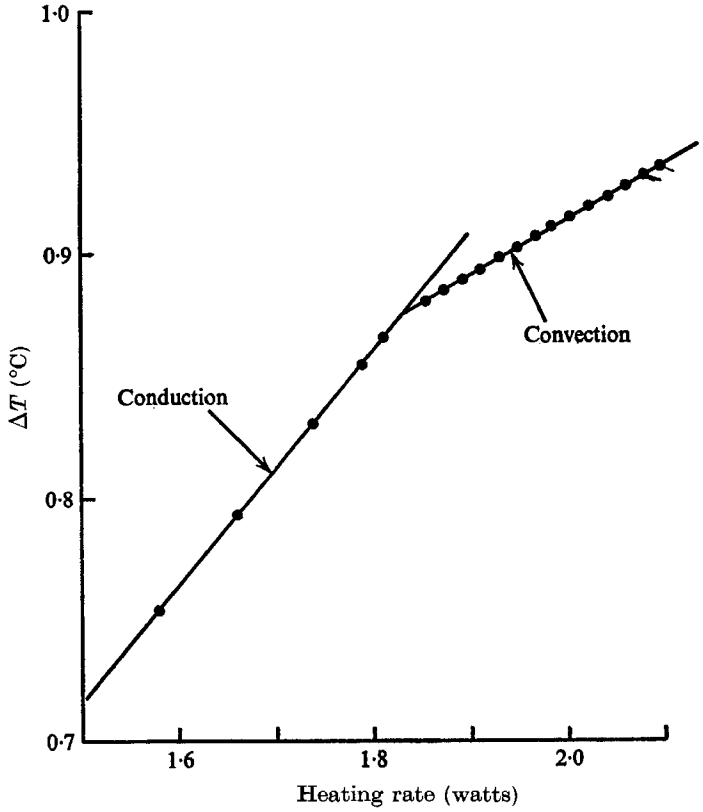

FIGURE 1. 'Classical' heating curve. ΔT, the temperature difference across the fluid layer is plotted against the total heating rate. The pressure was 826 bars.

This cannot have been the result of any experimental error; the precision in both measurements was 0·02 % or better, and this particular observation was repeated four times with nearly identical results. Subsequent small increases in Q did not increase ΔT; an increase of 30 % in Q was required to restore ΔT to the value it had before the drop. The apparent value of R_c at which this effect began was 2107. No transition was seen at lower Rayleigh numbers.

These observations seemed so interesting that somewhat more investigation was undertaken. Details of the apparatus, some heating curves, measurements of critical Rayleigh numbers, and some speculation are presented in this paper.

The apparatus

Because this device was designed for use with sea water at high pressures, some features of it had to be a little different from previous Rayleigh–Bénard experiments. The essential part is a horizontal fluid layer bounded top and

bottom by parallel plates; the top plate is cooled and the bottom plate heated. Since the critical Rayleigh number was calculated for the horizontally infinite case, the width-to-height ratio of the fluid layer should be large (28 for this device, 15–135 for Silveston's, 16 for Malkus's, 25 for Schmidt & Milverton's). The plates must be maintained parallel and the separation kept constant (or known) as the pressure and temperature are changed. Quartz is used to separate the plates because of its low compressibility, thermal expansion, and thermal conductivity. As shown in figure 2, the top plate rests on three 0·635 cm quartz spacers, (*b*), and slides freely on the rods which support the device from below. Plate separation varies by less than 0·1 %. The plates are maintained parallel to within 20 seconds of arc.

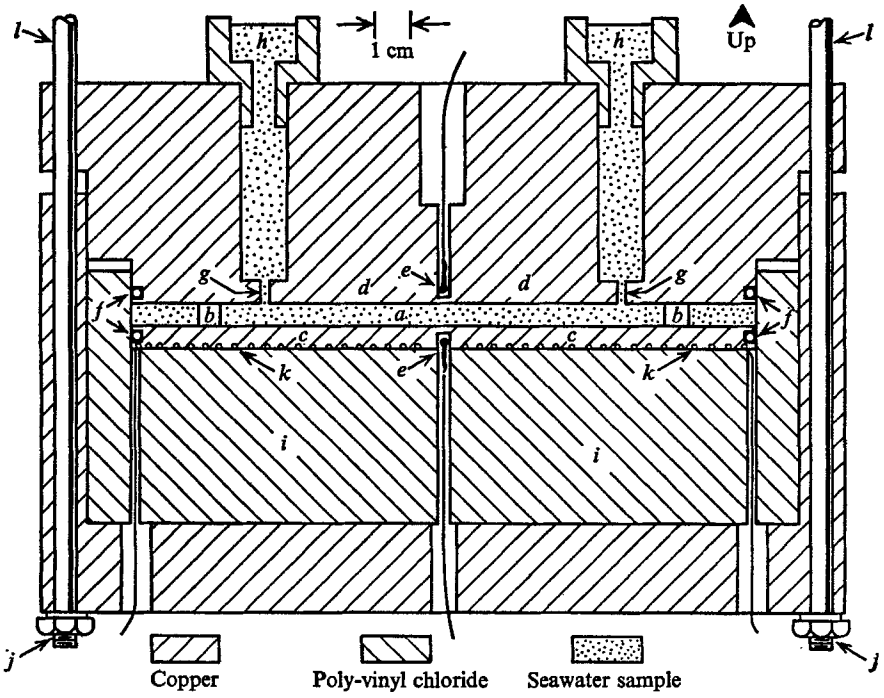

FIGURE 2. The apparatus as placed inside the pressure bomb. The depth of the fluid layer, (*a*), is kept constant because the top section, (*d*), slides freely on rods, (*l*), and rests on quartz spacers, (*b*), which change their dimensions very little as the pressure and temperature are changed. Copper plate, (*c*), is heated by resistance wire placed in spiral grooves, (*k*) in its bottom. O-rings (*f*), keep the fluid from mixing with the hydraulic oil which surrounds this device. Reservoirs, (*h*), and tiny holes, (*g*), provide a way of loading the sample, and allowing for density changes. Thermistors, (*e*), measure the temperature of plates (*c*) and (*d*). The bottom plate, (*c*), is insulated below and at its sides by P.V.C., (*i*). The whole device rests on nuts, (*j*), at the bottom of the supporting rods, (*l*), which are threaded into the bomb top (not shown). This whole device, in its pressure bomb, sits in a temperature bath.

Heat flow

The pattern of heat flow is critically important. Horizontal heat flows (caused by external sources, the separation between the wires of the heating coil (*k*), the heat loss from the edges of the fluid, the difference in conductivity between the

quartz and the fluid, or any other asymmetries) will produce horizontal temperature gradients which might induce motion in the fluid. The vertical components of such motion might conduct enough heat to obscure the change in slope of the heating curve due to the Rayleigh–Bénard instability and might even represent sufficient perturbations of the initial state that the theory would no longer apply. For each of these effects, however, the ratio of the horizontal temperature variation to ΔT is less than the ratio of the thermal conductivities of the fluid and the plate. Copper, plated with nickel to inhibit corrosion, was used for the plates for this reason. The device is surrounded at sides and bottom by 1·27 cm of copper, and the shielding effect of the pressure bomb itself helps to reduce thermal gradients.

Ideally, the sides and bottom of the bottom plate would be made of perfectly insulating material so all the heat would have to flow vertically upward, through the fluid layer. Because this device was designed to be used at high pressures, however, good insulating materials, which would collapse under the pressure, could not be used. Poly-vinyl chloride was chosen for machining convenience and availability. The electrical leads to the coil and thermistors are very fine (no. 40) wire so that heat leak is minimized. Tests showed that 85 % of the heat goes through the fluid layer and 15 % is lost, mostly through the P.V.C. Current from a Hewlett Packard model 6112 regulated power supply (voltage regulated to 0·01 %) flows through the heating coil of Karma wire (resistance variation $< 0{\cdot}01$ %), so the accuracy in the calculation of power dissipated in the coil is 0·02 %.

The pressure-temperature system

A sixteen-inch naval shell was adapted for use as a pressure bomb by the addition of O-ring seals and electrical feed-throughs. Pressure was communicated by hydraulic fluid and measured with a Texas Instruments pressure gauge, to a precision of 0·01 bar. The gauge was factory-calibrated with a dead-weight tester. An error of one bar in pressure corresponds to an error of less than 0·25 % in R_c. Because the bomb contained almost all the fluid in the system, the only variations in pressure were those caused by variations in the temperature of the bomb.

The bomb was totally immersed in a water-bath. Well-stirred ice kept the temperature constant for the lowest-temperature runs, while mercury-in-glass relay was used to control bath heaters for higher temperatures. The bath temperature, measured with a Dymec crystal thermometer, could be held steady to within a few millidegrees during the course of a run. The slow thermal response of the bomb helped smooth out fluctuations.

Temperature measurement

The only measurements made in the course of the experiment which enter into the final calculation of R_c are ΔT and the mean temperature of the fluid, T_m. The temperatures above and below the layer are determined by Vee Co 32A11 thermistors mounted at the centres of the plates within 0·2 cm of the fluid. The temperature drop in the plates between this location and the fluid boundary is less than 0·03 % of ΔT.

Resistances were measured with a Leeds and Northrup Wheatstone Bridge and a Fluke null detector. By careful reading of the null detector, resistances could be read to 0·01 ohms out of total resistances of 2000–5000 ohms, so resolution in resistance was 0·0005 %. The temperature sensitivity of the thermistors was 3·8 % per °C so the resolution in temperature was about 0·1 millidegree.

Calibration required some care because the thermistors were not protected from pressure (although they are contained in glass probes) so their resistances were subject to change due to pressure as well as temperature. The resistance, r, of a thermistor at temperature T is commonly expressed:

$$r = r_0 \exp\left[\gamma(1/T_0 - 1/T)\right],$$

in terms of the resistance r_0 at temperature T_0, where the value of γ is characteristic of a given thermistor. (Temperatures here are in degrees Kelvin.) For each run the resistances of both thermistors were measured with no heat flow, as described below. This calibration data showed that pressure does not change γ significantly, but r_0 decreases as the pressure is increased at constant T_0. Since r_0 was measured for each run at T_0, with the thermistors at temperatures close to those to be used when ΔT_c was determined, thermistor accuracy depended mainly on the accuracy of the determination of γ, which was found by comparing r_0's from runs at different bath temperatures, i.e. fitting the formula for r above. The range in values of γ was 0·4 % of γ. The uncertainty, $E(T)$, in the calculated temperatures can be expressed in terms of the error in γ, $E(\gamma)$ as

$$E(T)/(T - T_0) = E(\gamma)/\gamma.$$

Then, if $T - T_0$ is less than 4 °C (it was usually much less), $E(T)$ is less than 0·02 °C. The uncertainty, $E(\Delta T)$, in ΔT is less: $E(\Delta T)/\Delta T = E(\gamma)/\gamma = 0{\cdot}4$ %. The mean temperature of the fluid was taken as the temperature of the top thermistor plus $(\frac{1}{2}\Delta T)$. The uncertainty in the absolute value of T_m is then 0·02 °C and that in the absolute value of ΔT is 0·4 % of ΔT. It should be remembered that the *precision* of the measurements is a great deal better than this.

The sample of sea water used as the fluid layer was prepared according to the formula given by Lyman & Fleming (1940) for 19·00‰ chlorinity (34·325‰ salinity). At the conclusion of the experiments, the salinity was determined by the Data Collection and Processing Groups at Scripps Institution of Oceanography by means of an inductive salinometer, to be 34·702‰. The precision of this salinometer is 0·005‰, which corresponds to an error in β of 0·03 %. As expected, the salinity increased because of evaporation of water as the sample was loaded under vacuum. (Salinity is defined as the total solid material in grams contained in 1 kg of sea water.)

Soret effect

When a temperature gradient is established in a solution, a diffusive solute flow starts, and if the system is allowed to come to mechanical equilibrium, a solute gradient will result (DeGroot 1952, p. 273). In our case, salt will flow from the warm regions at the bottom of the layer to the colder regions near the top. The

magnitude of the gradient thus established depends on the Soret coefficient, σ_T:

$$\sigma_T = \frac{1}{S}\frac{\Delta S}{\Delta T}, \quad \Delta S = \sigma_T S \Delta T,$$

where S is the concentration (salinity in ‰), ΔT is the temperature drop, and ΔS is the concentration change. The relative density difference produced, $\Delta\rho/\rho$ is

$$\frac{\Delta\rho}{\rho} = \frac{1}{\rho}\left[\frac{\partial\rho}{\partial S}\right]_{P,T}\Delta S = \sigma_T \frac{1}{\rho}\left[\frac{\partial\rho}{\partial S}\right]_{P,T} S\,\Delta T.$$

The Soret coefficient has not been measured for sea water. Snowden & Turner (1960*a*, *b*) have made very accurate measurements in dilute (< 0·05 molar) solutions of NaCl and some other common salts, but only at temperatures of 15 °C and above. Longsworth's (1957) work on KCl at concentrations of 1 molar and above shows a very large temperature dependence of σ_T. The sign of σ_T as defined here is usually negative; that is the solute usually flows from hot areas to cold areas, in the same direction as the heat flux. Thus, when a solution is heated from below, the solute will migrate upwards, thereby having a destabilizing effect by increasing the vertical density gradient. It is possible, however, for σ_T to have a positive sign. Snowden & Turner (1960*a*) found positive σ_T for potassium iodide and lithium iodide at 0·01 molar concentration, 25·3 °C. Agar & Turner (1960) found that σ_T was negative at 25 °C in dilute NaCl, but its rate of change with temperature is so rapid that if their values at 25 °C and 35 °C are linearly extrapolated to 0 °C, they yield a positive value. Longsworth's measurements on KCl show a similar effect: from his figure 8 it seems clear that σ_T changes sign between 10 °C and 20 °C for 1 and 2 molar solutions. It seems quite possible, then, that σ_T may be positive in salt water at low temperatures, and that the stabilization at low values of $\Delta\beta/\beta$ observed may be due to a stabilizing salt gradient. More needs to be known about the pressure and temperature dependencies of the Soret effect before its effect on stability of salt water can be determined. It might be noted that an increase in salinity increases the thermal expansion coefficient, opposing the effect of the temperature gradient in this respect.

Procedure

One experimental run was accomplished as follows: (1) The temperature of the water-bath and the pressure in the hydraulic system are set. No heat is supplied to the bottom plate. (2) An overnight wait allows the system to come to equilibrium. (3) The pressure, the temperature, and the resistances of the thermistors are recorded for calibration. (4) The heating current is set to supply heat flow somewhat less than necessary for convection. (5) We wait for transient effects along the path to die away. (6) Thermistor resistances are read and converted to temperatures. (7) A point is plotted on the ΔT *vs.* heat flow plot (figure 1). (8) Heat flow is increased slightly and, after a wait for steady-state conditions, steps (6) and (7) are repeated. (9) When the change in slope of the plot is clear, the next run is begun.

Care was always taken to advance the heat flow slowly; ΔT was not increased by more than 1 % per hour on the average during a run.

Determination of T_c

The determination of the temperature, ΔT_c, at which convection begins, can be made from plots like figure 1. The procedure is to draw a straight line through the points at lower temperatures and one through the points above the estimated ΔT_c. The intersections of these lines is chosen as the point of onset. The range of choice is almost always less than 1 %. When the plot showed hysteresis, ΔT_c was taken as the temperature at which the first deviation from the conduction line was observed, on the path of *increasing* heat flow.

Observations

There are four major differences between the 'anomalous' transitions found when the pressure and temperature both were low and the 'classical' transitions found at high pressures and at high temperatures: (1) The shape of the heating curve was qualitatively different near transition. (2) Hysteresis in the heating curve was found. (3) There were oscillations in ΔT as Q was held constant just above transition. (4) The Rayleigh number for transition is larger than predicted by the simple theory. Each of these will be considered below.

Shape of heating curve

Figure 3 shows a heating curve for one very carefully done run. So many steps in Q were taken near transition that only a few can be shown in this plot. A section of the same plot is shown as figure 4 so that more detail can be seen, but still all points cannot be plotted. For $Q = 5{\cdot}92$ W, the points lie on the conduction line. As Q is increased past 5·92, ΔT drops by about 60 millidegrees (resolution in ΔT is 0·1 millidegree). Due to the oscillations (discussed later) the measurements of ΔT in this region had to be long term averages. At $Q = 7$ W, ΔT is increasing again, and for $Q = 7{\cdot}5$ W the points seem to be lying on a straight line again. The overall shape of this curve is strikingly similar to the curve referred to previously in Busse's paper (also those of Veronis and Krishnamurti). It seems to be characteristic of finite-amplitude transitions.

Hysteresis

When Q is decreased from its maximum value in figure 4, the curve is not retraced. ΔT is always smaller on this path than it was for the same Q when Q was being increased. (It should be kept in mind that all measurements were taken in steady state conditions.) The maximum hysteresis in ΔT was 0·23 °C (8 %). After another region of negative slope, the conduction line is rejoined at a point 0·07 °C (2·5 %) below the original transition. The points reproduce the original conduction line to better than 0·1 %, so we can be sure that no instrumental difficulties have influenced our observations. On other runs large increases in Q past 5·92 brought the system into other states, always in the middle of the hysteresis loop shown. This hysteresis is similar to that observed by Caldwell & Donnelly

(1962) for Couette flow with large gaps. One could imagine that figure 6 in that paper would have resembled figure 4 here if the torque (analogous to the heat flow) had been the set parameter instead of the Reynolds number.

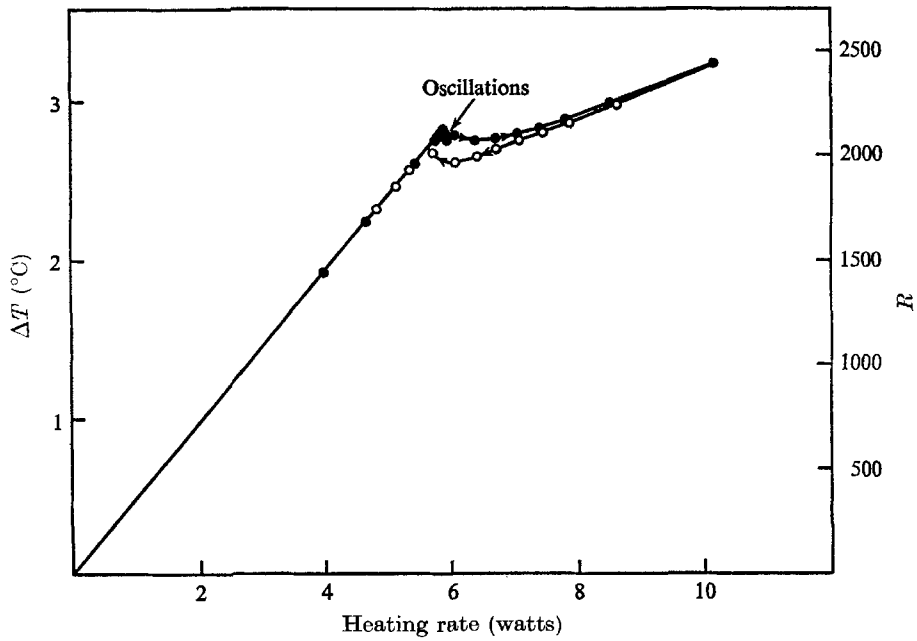

FIGURE 3. 'Anomalous' heating curve, at atmospheric pressure. ●, heat flow increasing; ○, heat flow decreasing.

Oscillations

When the heat flow is held constant just after transition (say, $Q = 6$ in figures 3 and 4), oscillations in ΔT are seen, as shown in figure 5. They are not sinusoidal, nor really very regular. The average period was about 20 min. Readings were taken (on digital magnetic tape) every 8 sec, so the individual points are not shown. These oscillations were watched for 48 h and did not appear to diminish in that time. Busse predicts relaxation oscillations at this point in the heating curve. No such oscillations were seen in the 'classical' runs; they would have had to be at least ten times smaller than those shown to escape observation.

Rayleigh number of the transition

For the 'anomalous' runs the observed critical Rayleigh number, which was calculated from the value of ΔT at which the first departure from the conduction line was observed as Q was increased, was higher than 1708. Because the runs for which the heating curves were 'anomalous' are just the runs where β is small and changing rapidly, R_c was plotted against $\Delta\beta/\beta$ in figure 6. $\Delta\beta$ is the change in β across the fluid layer due to the temperature difference. There seems to be a critical value of $\Delta\beta/\beta$ where Re_c starts to increase suddenly. Davis (1964) gives

the following formula for R_c when both fluid boundaries are free and the fluid properties vary:

$$R_c = 675[1 + 0{\cdot}175(\Delta k/k)\,(\Delta\beta/\beta) + 0{\cdot}02(\Delta\nu/\nu)\,(\Delta\beta/\beta) + 0{\cdot}135(\Delta k/k)\,(\Delta\nu/\nu) - 0{\cdot}0337(\Delta\beta/\beta)^2 - 0{\cdot}0965(\Delta k/k)^2 - 0{\cdot}047(\Delta\nu/\nu)^2].$$

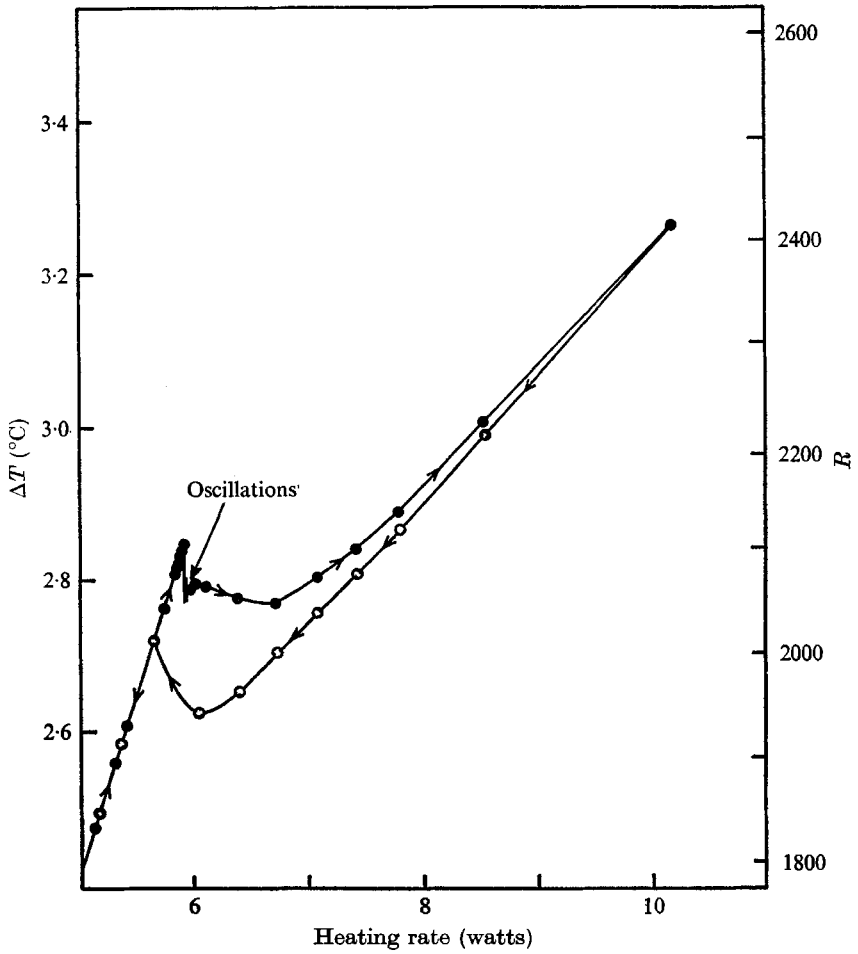

FIGURE 4. Same as figure 3 with change of scale.

This relation shows that R_c can be increased by variations in fluid properties across the layer, but not very much unless the variations are extreme. Actually, for the run shown in figures 3 and 4 a decrease of 0·3 % in R_c would be predicted, whereas an increase of 23 % is observed. It should be remembered that the boundary conditions used in the calculation of the formula are quite different from those of the experiment. The sudden increase in observed R_c means that the system is somehow stabilized against the effect of infinitesimal disturbances for larger curvatures of the density profile.

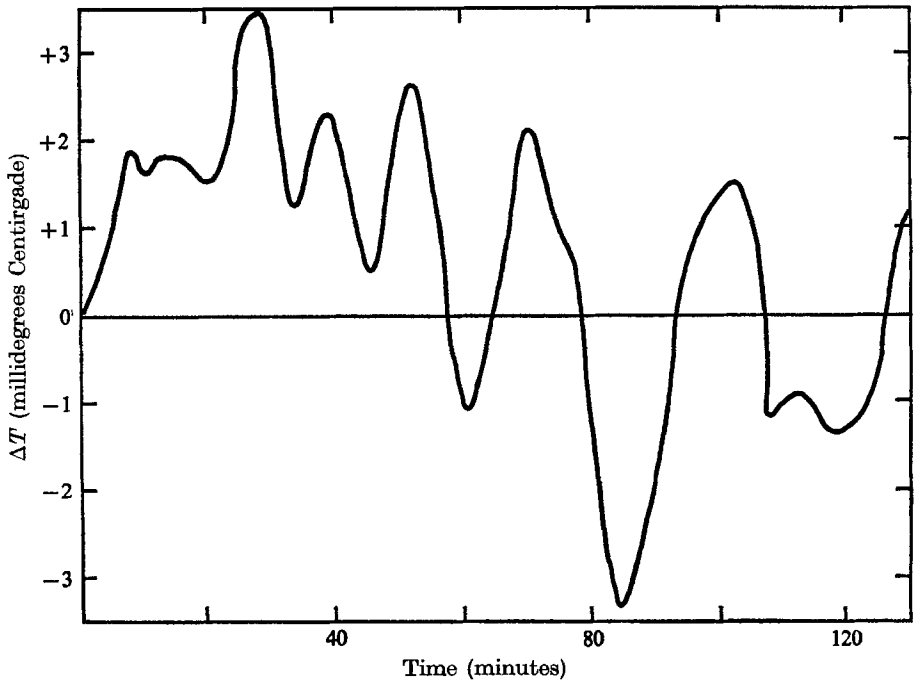

FIGURE 5. Deviation of ΔT from arbitrary values *vs.* time of day.

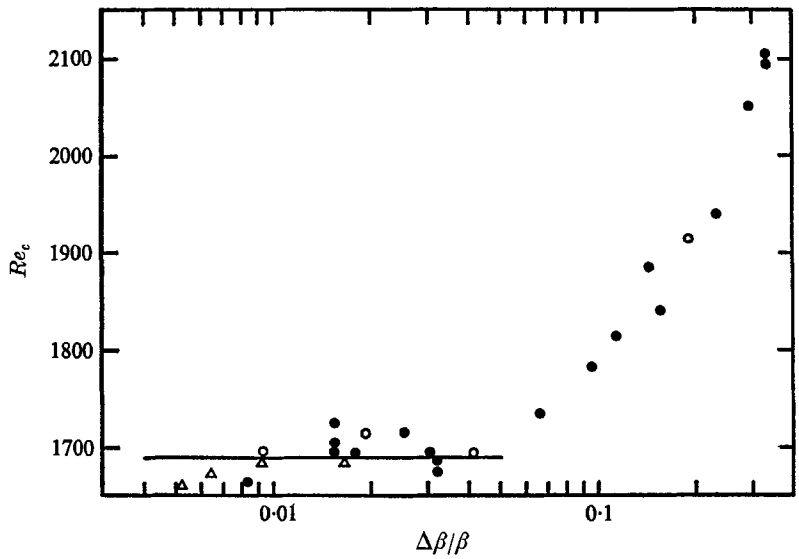

FIGURE 6. Apparent critical Rayleigh number *vs.* fractional change in thermal expansion across the fluid layer. ●, bath temperature 0 °C; ○, bath temperature 1·5 °C; △, bath temperatures 17·4 °C.

For the 18 runs where $\Delta\beta/\beta < 0{\cdot}05$, the mean value of R_c is 1690 with a standard deviation of 17·5 (1·04 %). The discrepancy between 1690 and 1708 is only 1·05 %, which is less than the uncertainty in the values of β used to calculate R_c. For $\Delta\beta/\beta > 0{\cdot}05$, R_c is linearly dependent on $\Delta\beta/\beta$: if $R_c = a + b(\Delta\beta/\beta)^n$, $a = 1656 \pm 5$, $b = 1333 \pm 35$, and $n = 1{\cdot}0 \pm 0{\cdot}013$ (these values were calculated by a least squares method).

Possible consequences of Soret-induced salt gradient

The solute Rayleigh number R_s, as defined by Veronis (1965) is

$$g[(1/\rho)\,\partial\rho/\partial S]_{P,T}\,(\partial S/\partial z)\,d^4/\nu x,$$

where S is the salinity. If the temperature gradient is maintained long enough for the Soret-induced salt gradient to be set up (3 h for our apparatus), R_s will be proportional to R, because $\partial S/\partial z = \sigma_T S(\partial T/\partial z)$:

$$R_s = \sigma_T S\,\frac{(1/\rho)\,(\partial\rho/\partial S)_{T,P}}{(1/\rho)\,(\partial\rho/\partial T)_{S,P}}\,.R.$$

For sea water at $S = 35‰$, $P = 1$ kilobar, $T = 0\,°\mathrm{C}$;

$$(1/\rho)\,(\partial\rho/\partial S)_{T,P} = 7{\cdot}0 \pm 10^{-4}\,(‰)^{-1}$$

and

$$(1/\rho)\,(\partial\rho/\partial T)_{S,P} = 3{\cdot}1 \times 10^{-4}\,°\mathrm{C}^{-1}$$

so

$$R_S = 80\,.\sigma_T\,.R.$$

If σ_T is negative, as is usual at room temperature, R_s is negative and the effect of the salt gradient is destabilizing. Nield (1967) uses the parameter

$$S^* = -(x/D)\,.R_S.$$

For the above conditions $S^* = -100R_S = -9 \times 10^3\,.\sigma_T\,.R$. Figure 1 of Nield's paper shows the boundary of stability against linear perturbations in an R, S plane. A layer of fluid in Soret equilibrium is represented by a point on the line passing through the origin having slope $-8 \times 10^3 T$. The layer should become unstable for the value of R at which this line crosses the stability boundary. This value of R will be smaller than the critical R for no salt gradient ($S^* = 0$).

If σ_T is positive, which is quite possible at temperatures near 0 °C in NaCl, R_s is positive, and the effect of the salt gradient is stabilizing. In Nield's diagram the locus of the system will be a line of *negative* slope passing through the origin, and the critical Rayleigh number will be larger than for the no salt gradient. In figure 3 in Veronis's (1965) paper, the stability boundaries are plotted in a $\log(R/\pi^4)$, $\log(Rs/\pi^4)$ plane. The system in Soret equilibrium is represented on this diagram by a straight line, parallel to the asymptotic lines for the stability boundaries. For the conditions considered above, $R_s = 80\sigma_T R$, so if

$$1{\cdot}25 \times 10^{-4} < \sigma_T < 1{\cdot}4 \times 10^{-2} \quad \text{(reasonable values)},$$

this line lies between the asymptotic lines for steady and overstable linear purturbations. Instability may occur first as either infinitesimal overstable motions ($\sigma_T < 0{\cdot}67 \times 10^{-3}\,°\mathrm{C}^{-1}$) or steady finite amplitude motions ($\sigma_T > 0{\cdot}67 \times 10^{-3}\,°\mathrm{C}^{-1}$).

Without knowing the sign of magnitude of σ_T we cannot be more definite about its influence. It does not seem, however, that a salt gradient is influencial in this experiment, because (1) if the salt gradient is important, it should be destabilizing at the higher temperatures. This was not observed. (2) The stabilization observed was very well correlated with $\Delta\beta/\beta$: it is possible, of course, that σ_T happens to be correlated with $\Delta\beta/\beta$ in a similar fashion. (3) The initial mode of instability is definitely identifiable as non-linear because of the large jump in ΔT, and fairly large oscillations are observed, so it probably is an oscillatory mode (finite amplitude oscillatory modes are not predicted by Veronis). Veronis used boundaries dynamically free, but at constant salinity and temperature. This may not be sufficiently similar to the present case of rigid boundaries which are impervious to salt, with heat production below held constant. It is also possible that Soret-induced salt fluxes might have to be included in order for the equation to describe thermohaline flow in some situations.

Conclusions

(1) Heating curves of the type described by Busse are traced by a Rayleigh–Bénard apparatus if the variation of a property of the fluid (thermal expansion in this case) is large enough.

(2) Oscillations in temperature do take place, in the range in the heating curve predicted by Busse.

(3) There is hysteresis in the heating wave near transition; the state of the system is history-dependent.

(4) For changes in thermal expansion across the fluid layer greater than 5 %, the critical Rayleigh number is increased. Transition is not observed until R is as much as 30 % above usual critical value of 1708: the system has been stabilized against infinitesimal perturbations. It must be borne in mind that a stabilizing Soret-effect induced salt gradient might exist.

(5) The solute flux due to the Soret effect may be significant in thermohaline convection.

The results of this experiment leave some questions unanswered. Some of these can be answered theoretically, some probably only by further experimentation.

(1) *Does the salt play a role in these phenomena?* It is hoped that it will be possible to reassemble this same device (which had to be torn down and moved) and try fresh water at a temperature where the variation of β would be similar to that of the salt water used here.

(2) *How is the system stabilized against infinitesimal perturbations for large* $\Delta\beta/\beta$*?* This is a theoretical question, although further experimentation might aid in its formulation.

(3) *What is the effect of boundary conditions?* According to Busse, the fact that the heat production in a layer below the fluid, rather than the Rayleigh number, be the 'set parameter' is crucial. Unfortunately it is difficult to arrange truly unambiguous boundary conditions in a real experiment, but some information could be obtained by varying the heat paths above and below the fluid.

(4) *What happens if the curvature of the density profile is increased?* Even more striking effects might be seen by using fresh water just above the density maximum, or salt water below 0 °C.

Maurice Chevallier and Merlin Ingraham machined the apparatus and Brian Tucker helped continually with the experimental work. The experimental work was done at the Institute for Geophysics and Planetary Physics at the University of California, San Diego, under National Science Foundation Grant GA-849. While this paper was being written, the author was partially supported by National Science Foundation Grant GA-1452 at Oregon State University.

REFERENCES

AGAR, J. N. & TURNER, J. C. R. 1960 *Proc. Roy. Soc.* A **255**, 307–330.

BUSSE, F. H. 1967 *J. Fluid Mech.* **28**, 223–239.

CALDWELL, D. R. & DONNELLY, R. J. 1962 *Proc. Roy. Soc.* A **267**, 197–205.

CALDWELL, D. R. & TUCKER, B. 1969 *Deep Sea Res.* (in the Press).

CHANDRASEKHAR, S. 1961 *Hydrodynamic and Hydromagnetic Stability*. Oxford: Clarendon Press.

DAVIS, S. H. 1964 Dissertation, R.P.I.

DEGROOT, S. R. 1952 *Thermodynamics of Irreversible Process*. New York: Interscience.

KRISHNAMURTI, R. 1968*a* *J. Fluid Mech.* **33**, 445–456.

KRISHNAMURTI, R. 1968*b* *J. Fluid Mech.* **33**, 457–463.

LAFOND, E. C. 1951 *U.S. Navy Hydrographic Publication* no. 614.

LONGSWORTH, L. G. 1957 *J. Phys. Chem.* **61**, 1557–1562.

LYMAN, J. & FLEMING, R. H. 1940 *J. Mar. Res.* **3**, 134–146.

MALKUS, W. 1954 *Proc. Roy. Soc.* A **225**, 185–260.

NIELD, D. A. 1967 *J. Fluid Mech.* **29**, 545–558.

SCHMIDT, R. J. & MILVERTON, S. W. 1935 *Proc. Roy. Soc.* A **152**, 586–594.

SILVESTON, P. L. 1958 *Forsch. Ing. Wes.* **24**, 29–32, 59–69.

SNOWDEN, P. N. & TURNER, J. C. R. 1960*a* *Trans. Faraday Soc.* **56**, 1409–1418.

SNOWDEN, P. N. & TURNER, J. C. R. 1960*b* *Trans. Faraday Soc.* **56**, 1812–1819.

VERONIS, G. 1963 *Astrophys.* **137**, 641–663.

VERONIS, G. 1965 *J. Mar. Res.* **23**, 1–17.